

Celt Report 18

California **E**xtrremely **L**arge **T**elescope

PRIMARY MIRROR ACTUATORS

**PHASE I STUDY
REPORT**

**Kenneth R. Lorell
Jean-Noel Aubrun**

Advanced Control and Systems Development

TABLE OF CONTENTS

1. Background	5
2. Concept Options	13
3. Concept Selection	19
4. Performance Analysis	27
5. Cost Estimate	41
6. Areas of Concern	42
7. Conclusions and Recommendations	44

1. Background

Substantial experience exists in the design and operation of the position actuation systems for the segments of segmented mirror telescopes. The aerospace industry, through programs like LODE (Large Optics Demonstration Experiment) and LAMP (Large Active Mirror Program) has experimented with actively-controlled large segmented mirrors since the early 1970 s. More recently, large astronomical telescopes, both terrestrial and space borne, have been proposed utilizing segmented mirrors. The Large Deployable Reflector is a somewhat dated NASA concept for a large orbiting infrared telescope and the Next Generation Space Telescope, the successor to the Hubble Space Telescope, will have a segmented 6 m primary mirror that can deploy in space.

The most credible experience with mirror segment actuation, however, has been gained by the designers of the 10-m Keck telescopes. These telescopes each use 108 actuators to position 36 primary mirror segments. The Keck telescopes have been highly successful, both from an engineering as well as scientific point of view, and have proven the concept of actively-controlled segmented mirrors as a useful technology for building large optics. The Keck segment positioning actuators are reliable and able to meet demanding performance requirements.

Given that the Keck actuators represent proven technology and have a track record of reliable operation under real-world conditions, it would seem logical to develop a CELT actuator based directly on the Keck design with only minor upgrades and improvements. Although this is certainly an option for CELT, this study will show that there are probably other approaches to the design of a segment positioning actuator that can provide better performance with higher reliability at lower weight, complexity, and cost than the Keck design. Because CELT will require 3000 segment actuators for operational conditions, and a total of 4000 actuators (including spares), the size, weight, cost, reliability, and power consumption of an individual actuator becomes substantially more critical for CELT than these considerations were at the time the original Keck actuators were designed nearly 15 years ago. This report will develop the design rationale for a CELT actuator and provide analysis and preliminary calculations to substantiate the proposed concept.

1.1 The Rigid Actuator

The Keck Ten Meter Telescope employs a hybrid motorized screw design that has proved highly successful under actual operating conditions. The Keck actuators are generically referred to as rigid actuators because of their extremely high axial stiffness. They operate by converting the rotary motion of a stepper motor through the use of a lead screw into the linear travel required to move the segment. The motor output is reduced by a gearbox before driving a rotating recirculating ball nut. The rotation of the nut causes the screw to move and subsequently apply pressure to a hydraulic bellows. This hydraulic device acts as an additional 36:1 gear reduction which permits the actuator to achieve a resolution of 4 nm per motor step. A preload spring has been incorporated in the top end of the actuator so that there can be no mechanical backlash as the load on the actuator changes with telescope elevation angle. This type of actuator is the equivalent of a rigid connection between the mirror whiffle tree and the mirror cell structure.

One of the main attractions of the rigid actuator is the apparent simplicity of operation with respect to the segment control system. The mirror segment control system commands each individual actuator to move an incremental distance once each control cycle. There are no

dynamic interactions between the mirror segment, the actuator, the mirror cell structure and the control system. The actuator behaves like an adjustable fixed mounting point between the whiffle tree and the structure. In fact, if the environmental disturbances were small enough, or the telescope were sitting still, the actuators could be turned off. This concept has great appeal for designers confronting the task of controlling such a large electromechanical system. Dynamically, the system of segments and rigid actuators looks like a set of mirrors sitting on static supports that can be periodically adjusted by remote control using a computer.

Unfortunately, it is extremely difficult to build a rigid segment positioning actuator whose positioning requirements are in the nanometer regime. The difficulty at this level of incremental motion is that the mechanical problems associated with friction, stiction (Coulomb friction), hysteresis, creep, thermal distortion, and other nonlinearities cause the actuator to have a substantial stochastic component to its operation. A command of x nm can never be achieved repeatably because the nonlinear mechanical properties of the actuator mechanism do not allow the rotation of the motor to translate into a repeatable, consistent motion of the output shaft.

The Keck actuators at least partially overcome this limitation by clever design. Use of extremely high gear ratios, a precision lead screw combined with the bellowfram, along with closed loop control on the motor rotation, allow the Keck devices to achieve reasonable performance. The price for this level of performance is complexity, weight, and high cost. It is estimated that at the time they were built in the early 1990 s, the Keck actuators cost about \$10,000 each. At this unit price, the CELT actuator set would cost \$40M.

In addition to problems fundamental to the mechanics of a rigid actuator, is the very property usually seen as an advantage to this type of device; the actuator's rigidity. That is, the rigid actuator directly transfers forces from the mirror cell structure to the whiffle tree and segment, and from the segment/whiffle tree back to the structure. Thus any disturbances from either direction, will eventually cause some level of mechanical excitation. Not only will the dynamics of the segment/whiffle tree and mirror cell be excited, but because the actuator has such high axial stiffness, there is no means of dissipating the energy. In fact, if the segment control system is not tuned correctly, the actuators will actually add to the vibrational energy and drive the system unstable. The Keck segment position control system avoids this problem using the basic control system technique of gain stabilization. That is, the gain, and therefore the operating bandwidth, is reduced to a level such that these problems do not occur. The current mode of operation of the Keck system is essentially quasi-static with an effective bandwidth of about 0.25 Hz.

1.2 The Soft Actuator

Another means of providing precise position control for a mirror segment is to connect the mirror to a high bandwidth actuation device such as a voice coil motor, similar to the main component of most loud speakers. This type of motor has no inherent mechanical stiffness, so unless electrical power is provided to the voice coil, the mirror segment cannot be supported. In order to make this type of motor work in a positioning system, a position sensor must be used to detect the position of the output shaft of the actuator relative to the actuator case and a local feedback control system is used to provide the exact amount of current in the voice coil so that the position sensor remains at the position commanded by the primary mirror segment-positioning control system.

The design concept of an actuator using a voice coil motor is a common approach to positioning electromechanical devices. It is relatively simple to implement, it can provide

high bandwidth control when necessary, it is lightweight, compact, relatively inexpensive, has very few moving parts, can move through a large mechanical range, is capable of large forces, and does not require lubrication. Most highly precise opto-mechanical systems, such as actively controlled mirrors used in telescopes and other optical applications, use voice coil motors for actuation. Both the Keck 1 and Keck 2 telescopes have active secondary mirrors (each with a different design), which use voice coil actuation, and the Gemini telescopes use an extremely complex voice coil driven secondary mirror, which not only provides optical alignment and focus, but also uses the same mechanism for chopping during infrared observations. The Boeing-Lockheed-TRW/USAF Airborne Laser system utilizes 14 large diameter beam steering mirrors, some of which have bandwidths in excess of 500 Hz, to precisely aim the high-energy laser and stabilize it in the presence of aircraft motion. Each of these mirrors uses voice coil motors to position the mirror when the system is in operation.

Voice coil driven actuators are referred to as soft actuators in contrast to the rigid positioning actuators such as the Keck segment actuators. Whereas a rigid actuator is sometimes thought of as set and forget, i.e., once the actuator has correctly positioned the segment, it can essentially be turned off (in theory) until a new segment position is desired. If there were nothing disturbing the position of the segments, a rigid actuator would really be set and forget. Actuation systems for focus, tip/tilt, and decenter of telescope secondary mirrors, especially for spaceborne optical systems, often utilize rigid set and forget actuators because the quiescent thermal and mechanical environment and relatively imprecise adjustment tolerances (microns, rather than nanometers) mean that the actuators are used on an extremely low duty cycle.

Since the segments of a segmented mirror terrestrial telescope are constantly subjected to motion of the support structure and disturbances from the environment, there is no real operational, power saving, or lifetime advantage to an actuator with set and forget capability. In effect, even though voice coil actuators must have electrical power and be functioning whenever the segment control system is in operation, as well as be monitored and positioned continuously by their local control loop in order to maintain precise position control, their operating duty cycle is really no different from the rigid actuator in a realistic operational environment.

Rigid actuators have the stiffness of a direct mechanical connection between the segment and the telescope structure. It is possible for them to have a stiffness value equivalent to a bolted interface. A voice coil actuator can achieve the same nearly infinite stiffness for disturbances at frequencies that are below 0.1 Hz or so, but as the frequency of the disturbance increases, the ability of the closed loop system controlling the voice coil to remain stiff decreases. Thus, the term soft actuator applies not only to the actuator in the non-operating condition, but also to the way the actuator responds to higher frequency disturbances. An analysis and comparison of rigid and soft actuators and how they affect the overall performance of the segment positioning system in the presence of structural vibration and segment disturbances is presented in Section 2 of this report. An interesting conclusion of this analysis is that some small, controlled amount of compliance in the actuator, when properly designed, is actually advantageous to the segment positioning system. Figure 1-1 illustrates a voice coil driven soft actuator with a control loop closed around a position sensor.

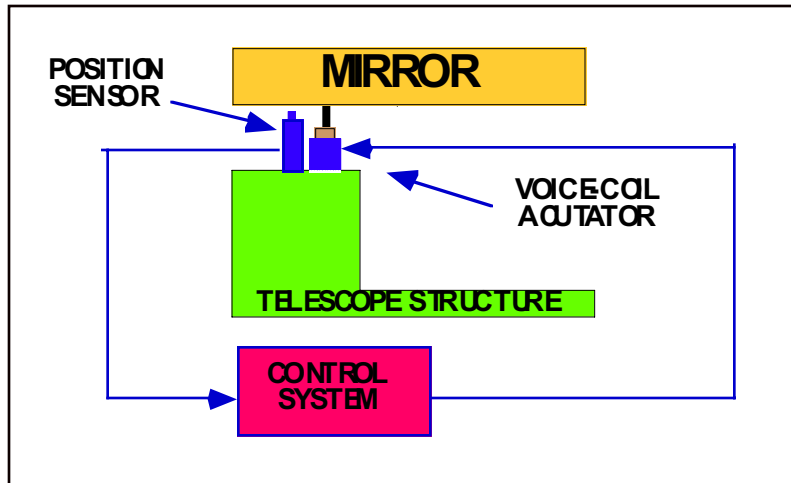


Figure 1-1: Voice coil driven soft actuator with closed loop control system

1.3 Gravity Offloading

A voice coil driven soft actuator used to position a terrestrial telescope mirror segment can operate with extremely low power only through the use of gravity offloading. Gravity offloading is a means of removing essentially all of the static force due to the weight of the mirror segment. Any segment actuator, regardless of design, must supply this static force. A rigid actuator, of course, is designed to support the full weight of the segment because it is essentially a rigid connection between the segment and the mirror support structure and thus does not require offloading. A soft actuator, however, must use some of its force capability to support the segment gravitational load, independent of other requirements related to mirror control dynamics. Offloading serves the purpose of simultaneously reducing requirements for both actuator power and force. An offloaded voice coil (of any capacity) not only uses less energy because it doesn't have to work as hard, it can also be substantially smaller than one designed for a non-offloaded system because it only has to provide forces associated with dynamic requirements such as repositioning the segment and correcting for mechanical, acoustic, aerodynamic, and other disturbances.

1.3.1 Passive Offloading

There are a number of means of providing gravity offloading. In general, there are two broad categories; passive and active offloading. Passive offloading utilizes a counterweight on a lever arm to exactly offset the weight of the segment. An interesting feature of a levered counterweight offloading system is that once the system is in balance, it remains in balance independent of the elevation angle of the telescope. Figure 1-2 shows a soft voice coil driven segment actuator that uses passive counterweights for offloading.

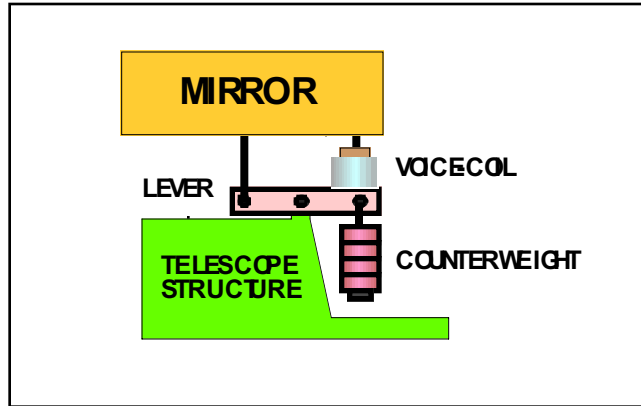


Figure 1-2 Passive counterweight offload for a voice coil driven soft actuator

1.3.2 Active Offloading

Active offloading can be divided into two sub categories; fully active and hybrid active/passive offloading. In either type of active offloading system, the amount of required offload is determined by measuring the static current in the voice coil actuator and adjusting the offload until the static current is driven to zero. Fully active offloading refers to providing the force required for offload solely by active means. In general, this implies that an auxiliary electric motor, for example, controls the extension or compression of a spring that applies the offload force. This motor is usually very small, operates at low speed and only intermittently, and requires a negligible amount of power. The motor is controlled to extend or compress the spring as a function of both the sign and magnitude of the DC value of the current in the voice coil actuator. Figure 1-3 illustrates a fully offloaded soft actuator.

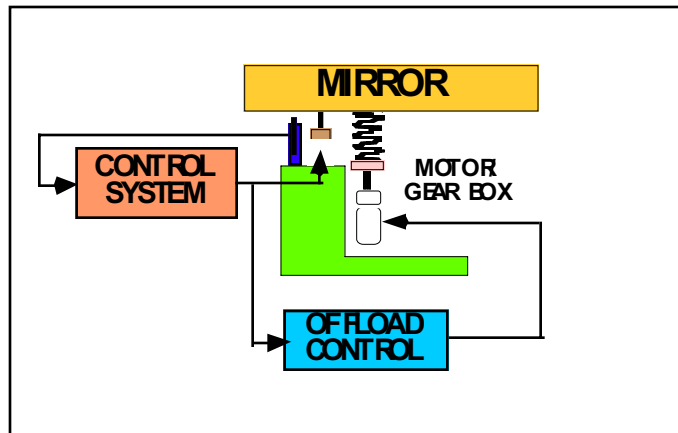
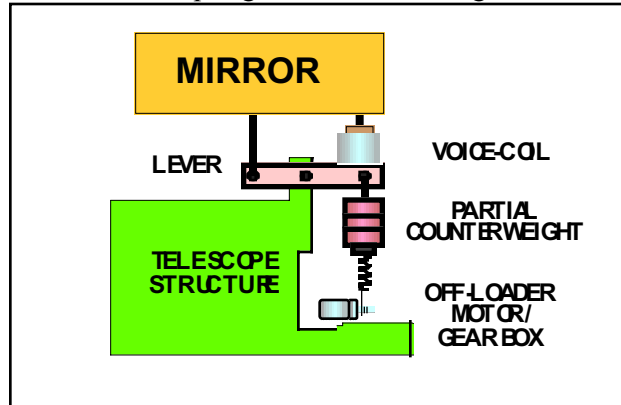


Figure 1-3 Fully offloaded voice coil driven soft actuator

1.3.3 Hybrid Active/Passive Offloading

Hybrid active/passive offloading is a variant of fully active offloading in which some, but not all, of the offload force is provided by a passive counterweight. The remainder of the offload is generated by an active system similar to that described in the preceding paragraph. The advantage of using a hybrid system is that the active part of the offload can be made to be extremely small and low power because it operates only as a trim to the primary passive offload. With respect to the all-passive system, a hybrid system does not require careful balancing of the offload counterweight because any imbalance is compensated for automatically by the active part of the system. The hybrid system will most likely be lighter

than a completely passive system because the counterweight (which only adds to the dead weight of the telescope system and can be substantial when a large number of segment actuators are required) can be smaller than in an all passive system. A hybrid offloading system using both a motor actuated spring and a counterweight is shown in Figure 1-4.



*Figure 1-4
Hybrid passive/active offloaded voice coil driven soft actuator*

1.4 Use of Levers for Actuator Force Advantage

In most segment positioning actuator designs, whether rigid or soft, the actuation device can benefit from some type of lever arrangement whose geometry provides a mechanical advantage or the device that generates the positioning force. Using a lever with a mechanical advantage allows the voice coil in a soft actuator to operate with a much lower required force. This permits

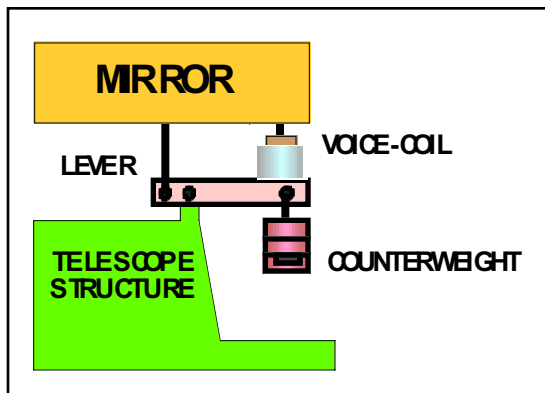


*Figure 1-5
Counterweight offloaded actuator
with mechanical advantage lever*

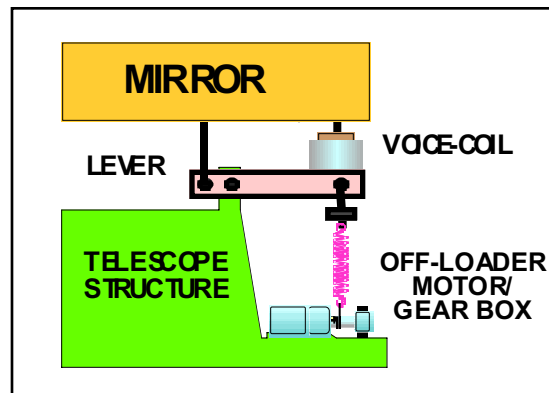


*Figure 1-6
Fully active offloaded
with mechanical advantage lever*

the use of smaller, lighter, lower-power actuators at the expense of a somewhat more sophisticated magnetic design for the voice coil itself. In addition to a smaller, lower-power voice coil, if the offload system can also take advantage of the lever geometry, the offload system can be smaller, lighter, and lower power as well. This applies to both the passive and active types of offload designs. In Figures 1-5 and 1-6, passive and active offloaded actuators using levers with mechanical advantage are illustrated.

1.5 Power Dissipation

In the preceding sections, the operation and design concepts for a soft actuator have been described. One of the key features of a voice coil driven soft actuator as compared with a rigid actuator is the continual use of electrical power. As discussed in Section 1.2, the rigid actuator in certain applications can actually be powered off while the soft actuator must remain powered under all operating conditions. However, later sections have illustrated, through the use of gravity offloading and the use of levers with mechanical advantage, how the soft actuator can minimize power consumption. In fact, because the segment positioning application requires that the segment actuators be continuously active whether they are of the rigid or of the soft variety, the electrical power dissipation of a correctly designed soft actuator utilizing a levered voice coil and offloader, can actually be as low or lower than a comparable rigid actuator. An estimate of electrical power dissipation is provided in Section 2 of this report.

1.6 Voice Coil Actuator Control Systems

Voice coil driven soft actuators are completely dependent on the use of a local closed loop control systems; one for the segment position control and one for active offloading. The architecture and design of these actuator control systems are the key to making the actuator meet performance requirements, be readily producible within a reasonable budget, and have acceptable reliability and operational lifetime. For these reasons, the analysis of the control systems and their impact on actuator sizing, duty cycle, segment control system performance, power dissipation, disturbance rejection, sensor requirements, and mechanical configuration takes up a major portion of this report. All of these subjects are examined in detail in Section 2

2. Concept Options

2.1 Requirements

The CELT Segment Positioning Actuators (CSPA) must satisfy a number of primary requirements that are listed below:

Range	> 1.2 mm
Rms. position error over 20 minutes	< 7 nm
Slew rate	> 10 $\mu\text{m/s}$ (full stroke in 2 minutes)
Transverse load capacity	> 5 Kg
Axial load capacity	> 30 Kg
Transverse stiffness	> 0.1 N/ μm
Axial stiffness	> 10 N/ μm (~ 100 Hz resonance)
Local average power dissipation	< 2 W
Lifetime	> 10 Years
Survival temperature	-18 to +22 °C
Operating temperature	-6 to +10 °C
Operating humidity	1 to 100% condensing

2.2 Design philosophy

The review of the requirements reveals the three most challenging items of the CSPA design:

- achieving a high position accuracy with a relatively large stroke, a dynamic range of almost 200,000/1.
- being able to operate with this accuracy under a load that can vary from zero to 30 Kg.
- keeping the axial stiffness high enough to sustain external disturbances without loss of accuracy.

Item c) is in fact equivalent to requiring that the system move less than 7nm under a 0.07 N disturbance. This number is important since it can be used to evaluate system performance in a more result oriented mode, the idea being that one could use other means (rather than straight mechanical stiffness) to achieve the same disturbance rejection result.

Similarly, it is seen from item b) that a 30Kg load change (i.e. 294 N) would produce a position variation of 29.4 μm given the required stiffness of 10 N/ μm . This variation is almost four orders of magnitude larger than the error budget of 7 nm. However this precision has to hold for only 20 minutes. If one assumes an average motion of the telescope of 15 arcsec/s (Earth rate), at 45 deg elevation, the actuator load change due to gravity is about 18 N, thus a position change of 1.8 μm . This number is still 260 times larger than the precision requirement.

A similar challenge arises from possible temperature variations. For example, a 30 cm long steel actuator will expand about 3.5 $\mu\text{m}/^\circ\text{C}$. Conversely, a temperature variation of only 2/1000 °C will produce 7 nm change.

For all these reasons, the mechanical design of the actuator must carefully address the positioning requirements as well as providing a clear definition of what actuator position really means. The cartoon shown in Figure 2-1 represents a simplified structural model of the actuator and the possible sensing schemes of the actuator position.

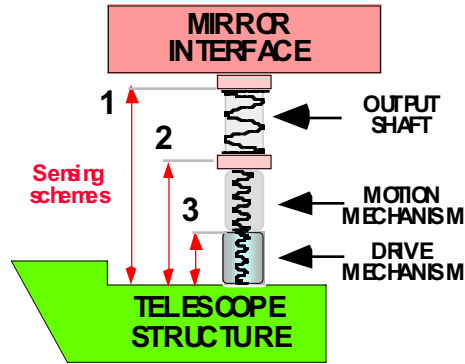


Figure 2-1. Actuator position sensing

In this representation, the actuator is made of three essential parts, an output shaft (relatively rigid) that transmits the motion to the mirror or mirror interface, a motion mechanism (e.g. screw drive), and a drive mechanism (e.g. motor/gear box). True sensing of the position is shown as #1, directly between the output of the actuator and a reference point on the telescope structure. If the output shaft is sufficiently rigid (and thermally stable) to satisfy the requirements discussed previously, then sensing can occur at the motion mechanism (#2). Often, sensing is simply provided at the drive mechanism itself (e.g. counting motor turns) which now requires more demanding performance from the motion mechanism (#3).

Accuracy requirements also have a direct effect upon the drive mechanism design which must have the correct resolution, accuracy and repeatability, and function under variable load conditions.

Additional considerations for the CSPA design include space and weight constraints, reliability and cost. The general philosophy of the design is thus to emphasize simplicity, direct actuation and sensing.

2.3 Basic concepts

2.3.1 Soft vs. rigid actuation

There are two basic approaches to position actuation:

1) The rigid actuation is one for which the motion is mechanically imposed (via gears, screws etc.). The position of the output shaft is thus purely defined by the kinematics and the stiffness of the system. In this case, external disturbance are attenuated in direct proportion to the system stiffness. However, this is only true for quasi-static disturbances. For time-varying disturbances, certain frequencies may be considerably amplified by structural resonances.

Using a simple spring/mass model for the actuator/mirror system with the $10 \text{ N}/\mu\text{m}$ required stiffness, and assuming a sinusoidal force disturbance of 0.05 N is acting on the actuator, one may calculate the position error as a function of frequency as shown in Figure 2-2. The amount of natural damping significantly affects the error at resonance, but not much so at lower frequencies. In this example, while the error is 5 nm at very low frequencies, it reaches 7 nm at 60 Hz , even with 2% natural damping, an already high value for a usual steel structure. In order to meet the requirements from zero to 100 Hz , the damping should be as high as 33% as shown on the bottom curve of Figure 2-2. This is not achievable practically with purely passive means.

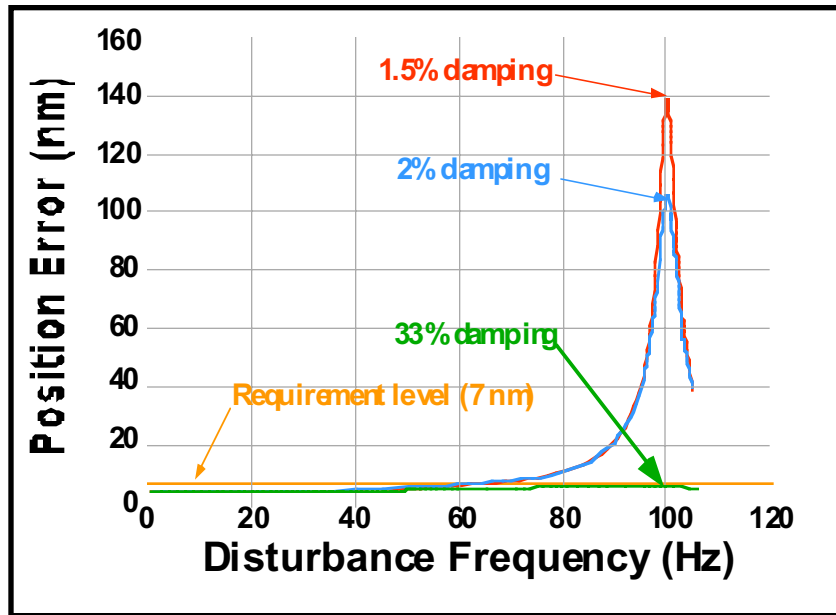


Figure 2-2. Position error for rigid actuator

2) In the soft actuation concept, the position is achieved by applying the correct force to the mirror. This force is adjusted constantly so as to maintain the desired position. Thus this type of actuation requires a control system which processes information given by a position sensor and generates the commands to the force actuator. When the control system is turned off, the system is generally exhibiting a very low natural stiffness. When the control system is on, the stiffness is caused by the control laws that essentially mimic the behavior of a spring (i.e. force proportional to displacement).

However, there is a significant difference in this case as far as the damping is concerned because the feedback loop can be used to introduce as much damping as is necessary. In other words, the control laws can mimic a dash pot as easily as it does a spring. Thus the 33% damping case shown in Figure 2-2 is achievable. In fact, in most optimal control systems, the damping ratio is usually set at 70% .

In addition, the spring and damping effects can be made dependent on the frequency. For example, in a classical PID control system, the stiffness is effectively infinite at zero frequency, meaning that no matter what constant load or thermal expansion is present, the position of the actuator is always the same. This presents a significant advantage over the rigid type, because the accuracy of the system is independent of external loads, thermal expansion, or any other inaccuracies and biases that may have been introduced mechanically.

Another very important feature of the soft actuation schemes is its ability to introduce damping in the overall system. To exemplify this property, we may consider a more realistic dynamical model for the mirror as shown in Figure 2-3. In this model, the whiffle tree is represented by a spring (K_w) between the mirror and the actuator output shaft. The actuator coil, spring and control system can be lumped into an equivalent spring/mass/damper system where spring and damping constants (K and D) are determined by the mass M of the interface and the control equation:

$$F_a = -G_p u - G_d du/dt \quad (1)$$

where F_a is the actuator force, G_p and G_d are proportional and differential gains respectively. The displacement u is measured by the position sensor of the control system. From the dynamic equation:

$$M \frac{d^2u}{dt^2} = F_a \quad (2)$$

one finds the relations:

$$K = G_p \quad (3)$$

$$D = G_d \quad (4)$$

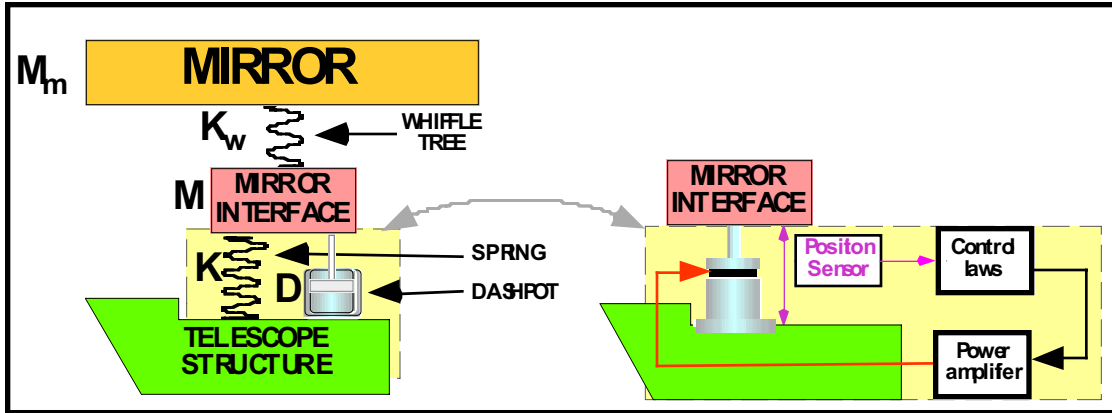


Figure 2-3. Soft actuator damping effect model

Adding the mirror and the whiffle tree results in a coupled system. Calling z the inertial displacement of the mirror, the full equations of motion are given by:

$$M \frac{d^2u}{dt^2} + D \frac{du}{dt} + (K + K_w) u = K_w z \quad (5)$$

$$M_m \frac{d^2z}{dt^2} + D_m \frac{dz}{dt} + K_w z = K_w u + F_e \quad (6)$$

where F_e is the external disturbance force acting on the mirror (e.g. wind).

The frequency response of the system can be calculated from Eqs. 5 and 6. In particular, the motion z of the mirror is given as a function of the frequency ω of excitation by:

$$z(\omega) = P(\omega) / Q(\omega) F_e \quad (7)$$

where:

$$P(\omega) = [-\omega^2 + 2j(\zeta\omega_o + \alpha\zeta_m\omega_m)\omega + \omega_o^2] / M_m$$

$$Q(\omega) = \omega^4 - 2j[(\zeta\omega_o + (1+\alpha)\zeta_m\omega_m)]\omega^3 - [(1+\alpha)\omega_m^2 + \omega_o^2 + 4\zeta\zeta_m\omega_o\omega_m]\omega^2 + 2j[(\zeta\omega_o + \zeta_m\omega_m)\omega_o\omega_m]\omega + \omega_o^2\omega_m^2$$

and:

$$\alpha = M_w / M, \quad \omega_o^2 = K / M, \quad \omega_m^2 = K_w / M_m, \quad 2\zeta_m\omega_m = D_m / M_m, \quad \text{and} \quad 2\zeta\omega_o = D / M$$

Equation (7) is plotted on Figure 2-4 showing clearly that the active actuator is able to damp the motion of the mirror/whiffle tree system, a feature that is not available at all with a rigid type of actuator as shown also on Figure 2-4. The response $u(\omega)$ of both rigid and soft actuators to disturbance force produced directly on the actuator are also plotted on Figure 2-4. It is seen that the soft actuator reduces the resonant mirror response by a factor 20. The following parameter values were used in this example:

Mirror/whiffle tree system: $M_w = 75 \text{ Kg}$, $K_w = 10 \mu\text{m/N}$, $\zeta_m = 0.01$

Actuator: $M=15 \text{ Kg}$, $\omega_0 = 691 \text{ rad/s}$ (110Hz), $\zeta=2$.

For the rigid actuator it was assumed that K was $10 \mu\text{m/N}$ and ζ was also 1%.

Thus it is seen that a soft actuator has in fact a dual purpose: one is to position accurately the mirror, the second is to provide damping to the otherwise undamped mirror/whiffle tree system.

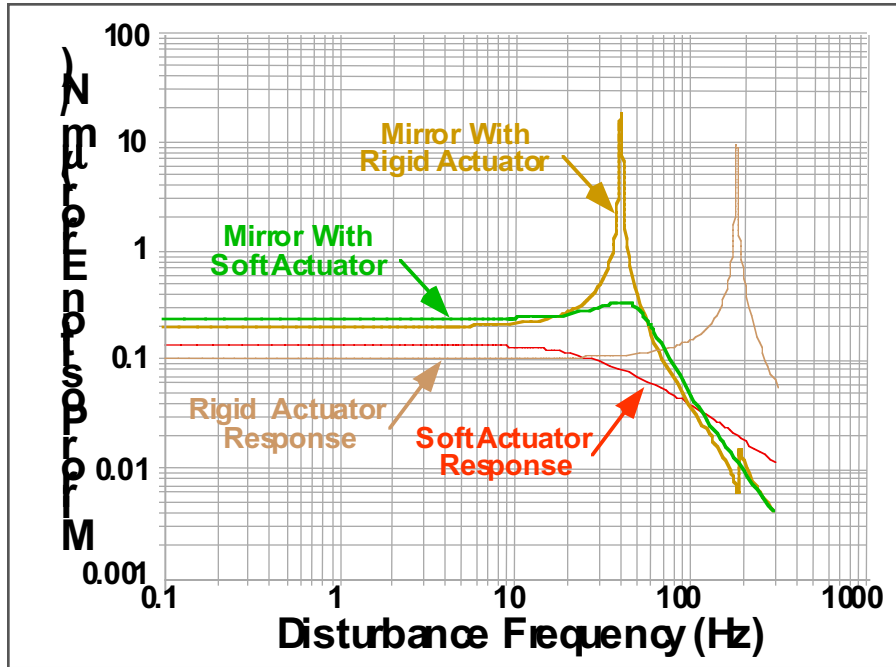


Figure 2-4. Mirror Response with Soft and Rigid Actuators

2.3.2 Off-loaded voice-coil concept

To combine the advantages of rigid actuators (which can hold a load without dissipating power) and soft actuators (which provide great accuracy and stability), the concept presented for the CSPA in this report uses a voice coil as the main position control actuator coupled with a mechanical off-load system.

The principle of such a system is shown in Figure 2-5. A spring, supporting the weight of the mirror, has its tension (or compression) adjusted by a motor/gear box/lead screw system to accommodate variations of the load due to changes in gravity vector as the telescope moves in elevation.

The spring/motor system provides approximately the force necessary to balance the applied load L . The voice coil actuator provides the remainder of the force (δL) plus a time-varying force (f) that provides the fine adjustment for all other disturbances and errors.

The control system reads the actuator position from a position sensor measuring the motion δx of the actuator shaft with respect to the telescope frame. Ideally this sensor is placed as close as possible to the mirror, but, as noted earlier, if the stiffness of the output shaft is large enough, this measurement can be made directly at the voice-coil actuator output.

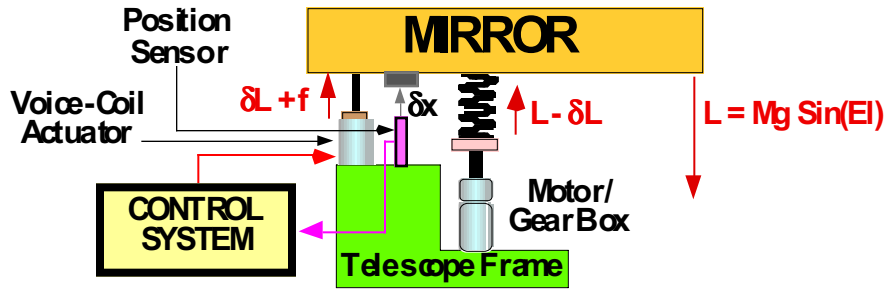


Figure 2-5. Off-loaded voice-coil concept

2.3.3 Active vs. passive offloading

If the mechanism by which the offloading is accomplished is of the generic type represented in Figure 2-5, the motor needs to be actively driven to follow the changes in gravity loads. The usual scheme is to use the voice coil drive current as the driving signal, so that the offloader motor is always trying to drive the voice-coil actuator current to zero. At zenith, the spring is compressed and supports the whole weight of the mirror. This load must be carried as well by the ball/screw gear box system, and the motor has to develop a reasonable amount of torque to handle this load.

One way to reduce the demand on the motor/gear/screw/spring system is to use a lever system as shown in Figure 2-6. With a 10:1 lever system for example, the design can be greatly simplified and use an expansion spring and a winch type actuation with a small motor.

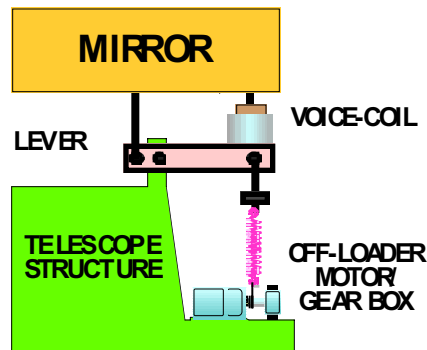


Figure 2-6. Active off-loading using a lever system

There is however another way to achieve offloading, which does not require motor or power. By using a passive counterweight, the mirror weight can be automatically balanced. This method has been used consistently in the past for balancing astronomical telescopes and offers indeed some advantages.

While an obvious disadvantage is the resulting increase in system weight, it is possible to significantly reduce this effect by using a lever system as shown in Figure 2-7. For example, a 10:1 lever ratio will result in a total weight increase of less than 10%. Also, if the voice coil actuator is connected to the lever as shown in the drawing, it is only required to produce one tenth of the force, resulting in lower power dissipation.

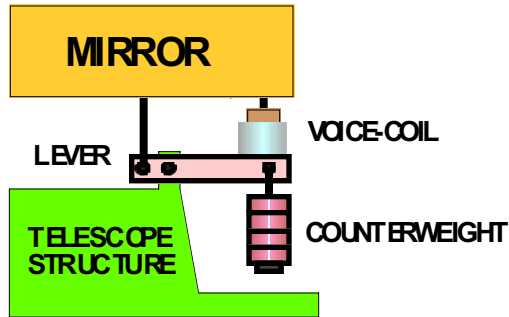


Figure 2-7. Fully counterweighted design

Such a design is very simple and robust, with a minimum of electronic and mechanical components. The position of the mirror is essentially independent of the gravity vector, so the voice coil actuator has very little corrections to perform to maintain position with high accuracy.

The drawback of this design is that it may require an adjustment of the counterweight for each actuator unit, to accommodate for possible manufacturing differences. If the weight unbalance error can be maintained below 10% for example, then the actuator would have to produce at most $10\% \times (1/10) \times 29.4\text{N}$, i.e. 0.3N (about an ounce). Given a typical voice coil producing 3 N/A with an electrical resistance of 2 Ohms, the steady power dissipation would be about 20 mW. This may still be too high and either the balance would have to be improved (a 1% error will now require less than 2 mW), or a hybrid active balancing system may be considered. as shown in Figure 2-8.

In this system, the offloader motor and offloading springs can be very small since they have to provide just a few ounces (as opposed to the full 294 N of a direct, non-counterweighted design).

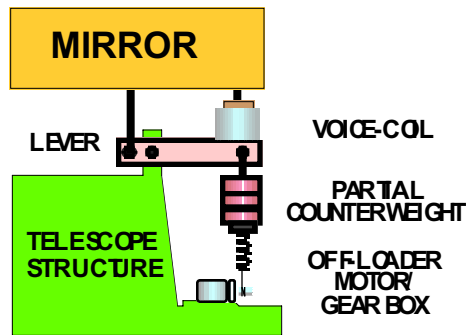


Figure 2-8. Partially counterweighted design with active offloading

3. Concept Selection

In section 2 a tradeoff between rigid actuators which provide a high degree of mechanical stiffness between the back of the mirror segment and the mirror support structure, and soft actuators which have no inherent axial rigidity but whose stiffness is a result of a closed loop control system was analyzed. The analysis indicated that there were a number of advantages to the soft actuator. These included lack of stiction and friction, no rubbing, sliding or lubricated parts, fewer overall components, capability for smoother, higher bandwidth control, and the ability to introduce damping not only of motions of the mirror segment, but of the support structure as well. As a result, the voice coil driven soft actuator is the basis for the design concepts recommended by this study.

3.1 Concept Description

Four actuator design concepts were developed, each of which utilized the offloaded voice coil as the primary control device. The concepts differ primarily in the way in which the offload is implemented. Although selection of a soft voice-coil driven actuator in comparison to a rigid actuator was the major design decision, the type of offload and its implementation have a substantial impact on the actuator design. The four concepts are described briefly below.

3.1.1 Concept A Direct Active Offload

The direct active offload design is shown as Concept A in Figure 3-1. In this design a motor-driven compression spring is used to provide gravity offload. Both the offloader and the voice coil are attached to the actuator output shaft directly without the use of levers. There are no counterweights. This design is relatively lightweight and compact but requires more force and torque from the voice coil actuator and the offload motor than other concepts.

3.1.2 Concept B Active Offload with Mechanical Advantage

Concept B in Figure 3-2 also uses a motor-driven spring for gravity offload. However, in this concept, the spring is of the extension type and both the voice coil and the offload motor act through a lever that provides a mechanical advantage. This design is relatively lightweight like Concept A, but cannot be built in as compact a package because of the lever geometry. The voice coil and offload motor can be substantially smaller and lower power than those in Concept A because of the lever arrangement.

3.1.3 Concept C Passive Offload with Mechanical Advantage

The third concept in Figure 3-3 does not use either a spring or a motor to provide offload. In Concept C, the offload force is generated by a counterweight acting through a lever. The voice coil acts through the same lever. This design has the largest and heaviest package of the four concepts, however, it is also the simplest, potentially the most reliable, and uses the least power. For optimum performance, it does require that the counterweight be carefully adjusted to exactly balance the load of the mirror segment and support hardware.

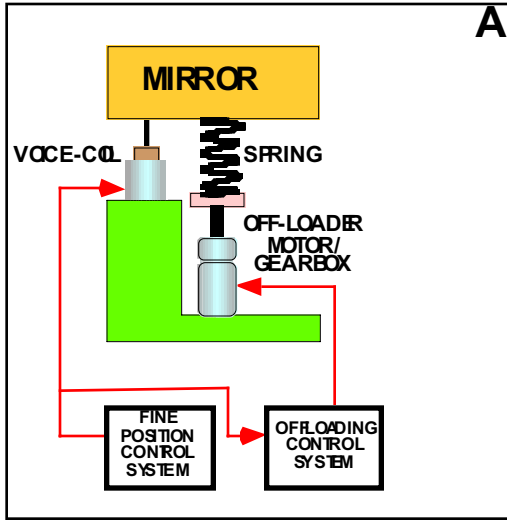


Figure 3-1 Concept A
Directly supported mirror with active offload

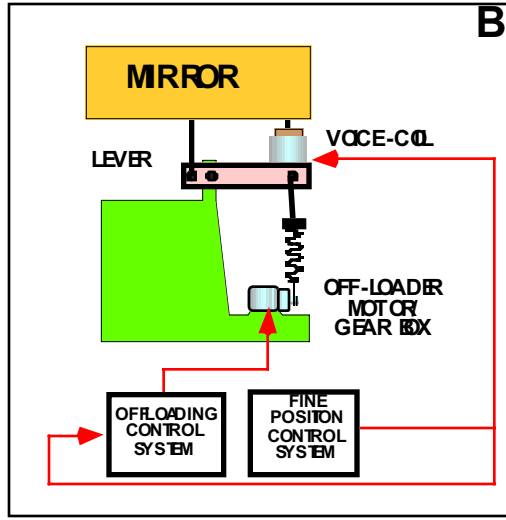


Figure 3-2 Concept B
Active offload with mechanical advantage

3.1.4 Concept D Hybrid Active/Passive Offload with Mechanical Advantage

Concept D, the last design shown in Figure 3-4 combines the features of Concepts B and C. A counterweight acting through a lever provides most of the offload force. In order to make the actuator lighter and remove the requirement for accurate adjustment of the counterweight after installation into the segment support system, Concept D also employs a motor-driven extension spring. By measuring the residual DC current in the voice coil actuator, the motor-spring system can automatically trim the offload force to the precise value that drives the current to zero. Because the combination of the partial counterweight and the lever system make the trim forces quite small, both the trim motor and spring can be compact, lightweight, and use very little power. Concept D has packaging volume requirements similar to Concept C, but is lighter weight.

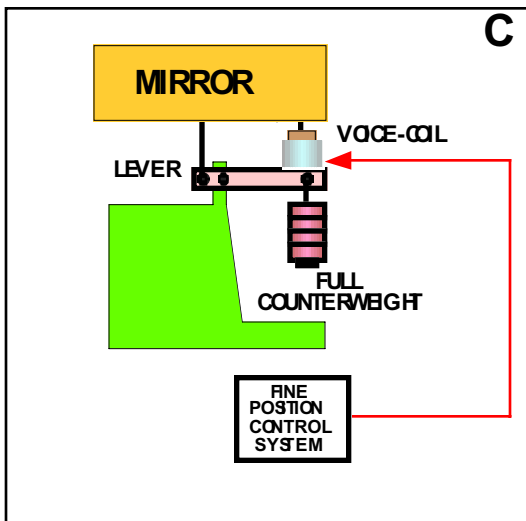


Figure 3-3 Concept C
Passive offload with mechanical advantage

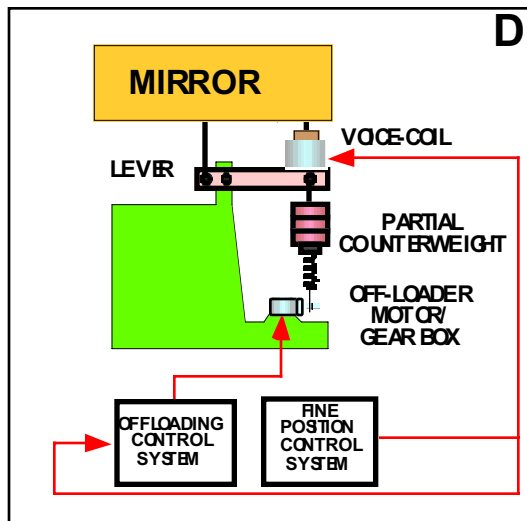


Figure 3-4 Concept D
Hybrid offload with mechanical advantage

3.1 Concept Selection Trade Table

A summary of the advantages and disadvantages of design concepts A through D is presented in table 3-1. Because each of the concepts utilizes a voice coil motor with a local position control loop to provide control for the segment position, the performance of the segment position control is assumed to be equivalent between the four concepts and is not considered in the trade. Features rated for each design include size, weight, cost, complexity, power, and reliability.

	SIZE	COST	WEIGHT	COMPLEXITY	POWER	RELIABILITY
A	smallest of 4 concepts	highest because of larger actuator and motor, plus screw drive for spring	lightest of 4 concepts - no counterweight	compression spring is hard to package	uses most power of 4 designs	least reliable because screw will wear
B	larger diameter than A	intermediate cost-need offload motor plus electronics but smaller than A	weight only slightly more than A because no counterweight and smaller voice coil	simpler than A but lever design is critical	uses less power than A but more than C and D	more reliable than A, same as D, and less than C
C	same package diameter as B and D, shortest of B C D	least expensive of 4 designs no active offload	heaviest of 4 designs -heavy counterweight	simplest of 4 designs- no active offload	lowest power of 4 designs lever plus no offload power is advantage	most reliable of 4 designs because has fewest parts and no active offload
D	same package diameter as B and C, same length as B	same cost as B, more than C less than A	heavier than B, less than C	same complexity as B	lower power than A and B, more than C	more reliable than A or B because less stress on motor

Table 3-1. Concept selection table

3.3 Design Recommendation

Advantages and disadvantages of each of the four design concepts are summarized in table 3.1 above. In this type of trade study it is extremely difficult to put a meaningful quantitative value on the ratings for each parameter, hence the rating process and the outcome of the overall selection tends to subjective.

Based on rating details in the table, two of the design concepts appear to have the most appeal for CELT. Selection of a specific concept may be influenced by system-level considerations. If the primary emphasis in the CELT design is simplicity and reliability, then Concept C, which utilizes passive-only offloading, is the clear choice. This design has the fewest mechanical parts, is completely fail safe (the offload is always in balance), and has the simplest electronic subsystem. It is also estimated to use the lowest amount of electrical power.

The problem with Concept C is that it is rather heavy and bulky because it requires a 3 kg counterweight. Although 3 kg does not seem excessive, CELT requires 3000 actuators which translates into at least 9000 kg of unproductive (non structural, non optical) weight on a moving component. This additional mass has impacts on the size of the rest of the structure (because the overall system weight will have to be even larger to accommodate the additional mass on the mirror cell), structural modes and frequencies, the sizing of the hydrostatic bearings, the AZ-EL drives, etc.

If the additional mass of Concept C is deemed excessive, then selecting any of the other three will require the use of active offloading which encompasses additional electronics, mechanism, and an electric motor. These elements will add power consumption, extra cost,

and reduce reliability relative to Concept C. Based on the evaluation in table 3.1, Concept D appears to be the best compromise. The reasoning behind this selection is that a reduced-size counterweight, which may be as small as 1 kg, can substantially reduce the size of the offload spring, motor, and gearbox. In addition, the smaller motor, spring, and gearbox will be lighter, less expensive, have smaller, less demanding mechanical loads, and use less power than those required for Concepts A and B. The package size of a Concept D design should be smaller than that for Concept C (but probably larger than for Concepts A and B) and weigh only slightly more, perhaps no more, than Concept A and B designs. These weights may be equivalent because the mass of the relatively small counterweight of Concept D is offset by reduced weight of the smaller spring and motor-gearbox compared with the equivalent hardware in Concepts A and B. Concept D should also have increased reliability compared with Concepts A and B because the offload mechanism is under less stress. In addition, because Concept D incorporates a counterweight, it does have some fail-safe capability, i.e., if the offload system fails, the actuator does have a much larger range of motion before the mechanism runs out of mechanical travel than either Concept A or B.

3.4 Mechanical Design

Based upon the previous considerations, a preliminary conceptual design was developed for the CPMA's as shown in Figure 3-5. One of the most important feature of this design is that it is absolutely *friction/stiction free* because all the motions are obtained through flexural elements.

Even though the offloading mechanism includes a motor/gear box system, the motion is transmitted through a very soft spring and its effects are entirely compensated for by the control system.

This design represents a significant departure from mechanical actuators that use any kind of bushings, bearings or screw drives. Three flexural levers arranged in a triangular configuration are attached, on one end, to an upper plate supporting the output shaft, and at the other end, to the counterweight. The three pivots are supported by the outside canister.

The size and weight of the counterweight can be adjusted from a minimum required for structural rigidity, to the full balanced value. A small extension spring connects the counterweight to the offload motor/gear box system. The choice for the spring stiffness is a function of the residual gravity unbalance after counterweighting the system.

The voice-coil actuator has its magnet mounted on the counterweight plate and its coil attached to the output shaft, thus the force it produces is amplified by lever ratio, with the magnet doing 90% of the moving. One reason for this mechanical arrangement is that the magnet becomes part of the counterweight, thus saving on the total system weight and power.

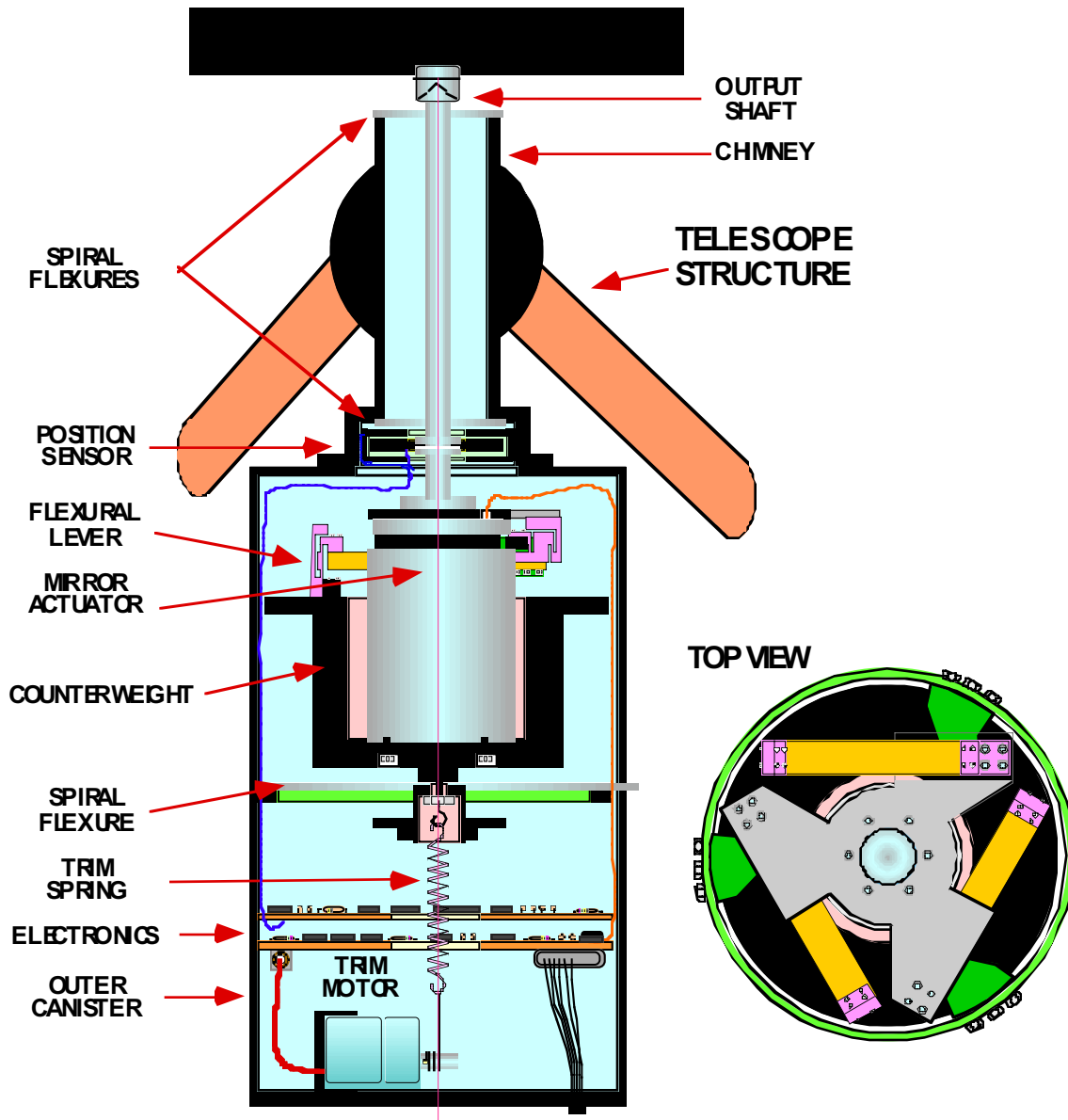


Figure 3-5 Conceptual Electromechanical Design

The output shaft is attached to two disk (spiral type) flexures which allow it to translate but provide enough rigidity in the transverse axis to satisfy the 5Kg , 0.1 N/ μ m requirements. The disk flexures are situated at both ends of a tube (chimney) which acts as a geometric reference for the actuator system and the interface with the telescope structure. The distance between the two flexures provides the rigidity required to handle the gravity couple resulting from the offset weight of the mirror/whiffle tree system.

The chimney is about 2 diameter and passes through a mounting hole inside a telescope structural node. The bottom part of the chimney is attached to the actuator's outside canister which contains all the mechanisms.

A detail of the flexural lever is shown in Figure 3-6. All the three flexures are under tension, thus avoiding buckling problems. Because in this case the flexures can be made thinner, the bending stresses are reduced, resulting in a significant increase in lifetime.

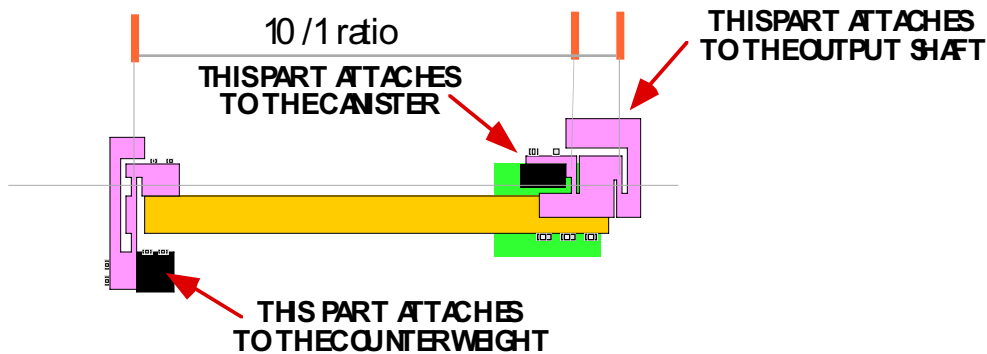


Figure 3-6 Flexural Lever Arrangement

The electronic boards are mounted inside the canister and are easily accessed through lateral doors. The details of the electronic design is given in the next section.

3.5 Electronic Architecture

The electronic architecture for the CELT actuator Concept D is shown in Figure 3.7. There are two separate control systems, one for the output position of the actuator, and one for the active/passive offload system. There is also a separate set of electronics for the capacitive position sensor that monitors the actuator position.

The sensor electronics are separated into a local electronics board that contains preamplifiers and is located immediately adjacent to the sensor capacitor plates and the remainder of the sensor electronics which is located on the same board as the rest of the control system. The reason for splitting the sensor electronics is that a local preamplifier greatly enhances the sensor signal to noise ratio and minimizes stray capacitance.

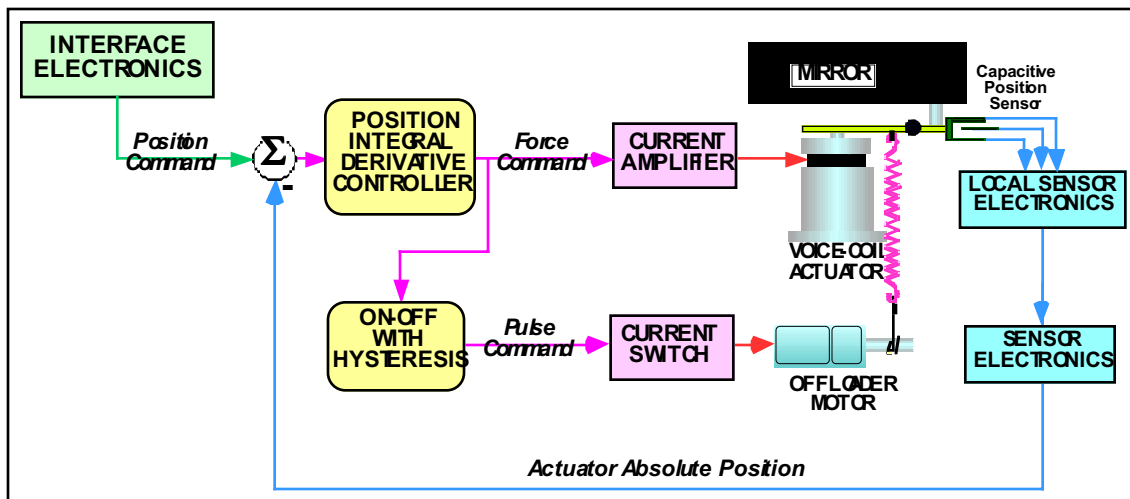


Figure 3.7 Actuator control system electronics block diagram

The actuator control electronics consist of the PID actuator position controller, the on-off offloader controller, power amplifiers for the voice coil and offload motors, and the position command decoding electronics.

The control of the offloading system is accomplished by a simple on/off logic. The average current in the voice-coil actuator is sampled at some low rate (10-100 /s) and compared to a bipolar threshold. When the threshold is exceeded, a pulse is sent to a current switch which drives the motor in one direction or the other for a very short time. This method is extremely efficient and requires a minimum of electronic parts.

All of the control system electronics, with the exception of the position command-decoding chip, are analog. They can be implemented using conventional off-the-shelf components on a printed circuit board. One option may be to package the electronics inside the actuator housing thereby eliminating cabling and connectors that add cost and reduce reliability.

4. Performance Analysis

This section describes the design and performance analyses of a soft, actively controlled, hybrid type actuator, which includes a voice coil actuator, a counterweight, an offloading spring, motor and gear box system.

4.1 Derived requirements

The proposed hybrid mirror position actuator (HMPA) concept contains a number of elements that must be calculated to meet the requirements of section 2. They are:

Item	Name	Units
- Lever ratio	L_r	unitless
-Voice Coil Actuator	.	.
Force constant	C_f	N/A
Power constant	C_p	N/root(W)
Coil Resistance	R	Ohm
Control bandwidth	ω_b	rad/s
-Counterweight		
Total mass	M_c	Kg
-Offloader spring	.	.
Spring constant	K_s	N/m
Unloaded length	L_s	m
-Gear Box	.	.
Gear Ratio	G_r	unitless
Output shaft radius	R_s	m
-Motor	.	.
Required torque	T_m	N.m
Max required rate	Ω	rad/s
Torque constant	MC_t	N.m/A
Power constant	MC_p	N.m/root(W)

Table 4-1 Main system parameters

A single actuator only sees (statically) a mass M_s equal to the third of the total mass of the mirror/whiffle tree system. This mass is given as 30 Kg in the requirements (approximately 25 Kg are due to the mirror itself, 5 Kg to the whiffle tree).

Nominal lever ratio	L_f	(nom 1/10)
Nominal force disturbance on mirror	F_d	(nom 1/3 N)
Max position error	dz_{max}	(nom 7 nm)
Minimum slew time (Z to H)	t_s	(nom 120 sec)
Total actuator stroke	Z_{max}	(nom 1.2 mm)

The following equations can be derived:

$$\text{Gravity load on voice-coil/spring system} \quad F_g = (L_r M_s - M_c) g \quad (4- 1)$$

$$\text{Required offloader motor torque} \quad T_m = 2\pi R_s F_g / G_r \quad (4- 2)$$

$$\text{Spring max extension (at horizon)} \quad X_{max} = F_g / K_s \quad (4- 3)$$

$$\text{Unloaded spring length} \quad L_s = 2 X_{max} \quad (4- 4)$$

$$\text{Output shaft max number of turns} \quad N_s = X_{max} / (2\pi R_s) \quad (4- 5)$$

$$\text{Motor number of turns (Z to H)} \quad N_m = G_r N_s \quad (4- 6)$$

$$\text{Motor maximum rate} \quad \Omega = N_m / t_s \quad (4- 7)$$

Minimum offloader force increment $\Delta F_{\min} = 2\pi R_s K_s / G_r$ (4- 8)

Max actuator required force $F_{\max} = K_s Z_{\max}$ (4- 9)

Nominal actuator required force $F_{\text{nom}} = (L_f F_d + \Delta F_{\min}) / K_s$
(4-10)

Nominal power consumption $W_{\text{nom}} = F_{\text{nom}}^2 / C_p^2$ (4-11)

Bandwidth required $\omega_b = 0.563 [F_d / (M_s dz_{\max})]^{1/2}$ (4-12)

These equations will be used to design and size various parts of the system as shown in the next few sections.

4.2 Motor, spring, gear box sizing

The choice of the spring constant and gear box ratio must be done first because they influence quite directly the design of the voice coil actuator. From Eqs. 4-1, 4-5, 4-6 and 4-7, one obtains two conditions to satisfy slew rate and motor torque:

$$\Delta_o > X_{\max} / (\Omega t_s) \quad (4-13)$$

$$\Delta_o < T_m / F_g \quad (4-14)$$

where Δ_o , is the linear gain of the motor/gear/winch system (in m/turn),

$$\Delta_o = 2\pi R_s / G_r \quad (4-15)$$

The spring constant can be determined independently from 4-3:

$$K_s = F_g / X_{\max} \quad (4-16)$$

Figure 4-1 shows the parameter space for Δ_o and T_m . The motor torque T_m is itself bounded by available motor characteristics.

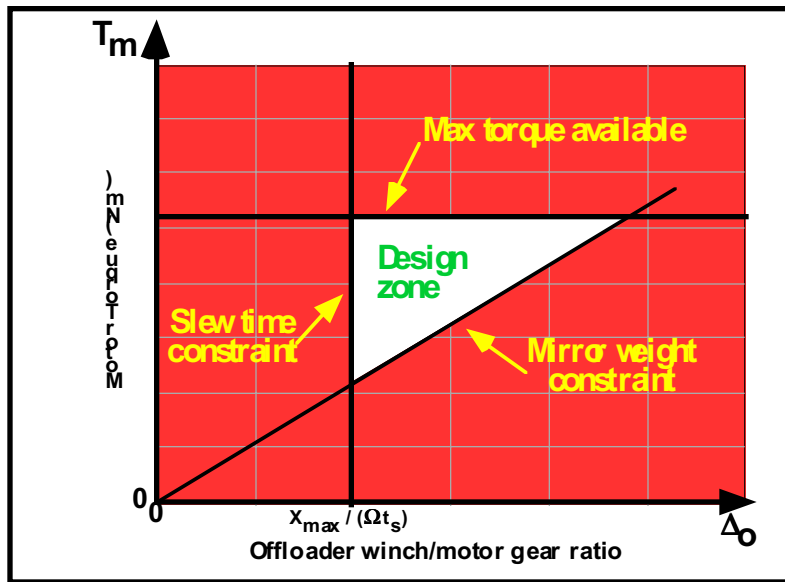


Figure 4-1 Gear and motor torque trade space

Using the following parameters:

$$\Omega = 105 \text{ rad/s (about 1000 rpm)}$$

$$t_s = 120 \text{ s}$$

$$X_{\max} = 60 \text{ mm}$$

$$\begin{aligned}
M_c &= 0 \text{ Kg} \quad (\text{worst case}) \\
F_g &= 0.1 * 30 * 9.81 = 29.4 \text{ N} \\
T_m &= 0.007 \text{ N.m} \quad (1 \text{ oz.in})
\end{aligned}$$

one determines that

$$4.77 \cdot 10^{-6} < \Delta_o < 2.410^{-4} \tag{4-17}$$

If only one turn is desired on the winch shaft (to avoid cable overlap), then:

$$R_s = 10 \text{ mm}$$

and 4-17 gives the range of values for the gear ratio:

$$252 < Gr < 12,566$$

In the baseline design, the gear ratio is thus chosen to be 2400:1.

(This corresponds to $\Delta_o = 26 \mu\text{m} / \text{turn}$)

And the spring constant is defined:

$$K_s = 29.46 / 0.06 = 490 \text{ N/m}$$

In the baseline design, the spring constant is thus chosen to be 3 lb/in.

4.3 Main actuator sizing

The voice coil actuator characteristics are chosen to satisfy the total stroke Z_{max} , the maximum force F_{max} (4.-9), and the power requirements (4-11) :

$$F_{\text{max}} = Z_{\text{max}} * K_s \tag{4-18}$$

$$W_{\text{nom}} = [L_f F_d + \Delta_o K_s]^2 / C_p^2 \tag{4-19}$$

Since K_s is known, the actuator force is immediately calculated

$$F_{\text{max}} = 0.012 * 490 = 6 \text{ N}$$

In the baseline design, the maximum actuator force is thus chosen to be 1.5 lbs.

The nominal power dissipation is now evaluated from 4-19:

$$W_{\text{nom}} = (0.0333 + 26 \cdot 10^{-6} * 490)^2 / C_p^2 = 0.002 / C_p^2$$

To achieve a goal of 1 mW max in normal operations, the desired motor constant of the actuator has to be $C_p > 1.4 \text{ N}/\sqrt{\text{W}}$. However, there is also the power dissipated in the electronics, especially the power amplifier. Although 1 mW in the coil is very small, it corresponds to about 22 mA of current in a typical 2Ω coil resistance. This current has to flow from a 15V power supply, thus a corresponding power loss of about 300 mW.

In the baseline design, the actuator power constant is chosen to be above 1 lb/root(W).

4.4 Control system design

The control system wrapped around the voice coil actuator uses an analog position sensor to determine the position of the actuator shaft. From this signal, the control laws generate a current command to the actuator so that the actuator position is maintained equal to a desired (commanded) position (Figure 4-2).

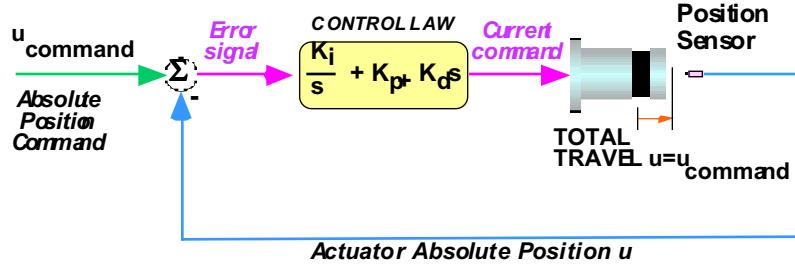


Figure 4-2 Position control system schematic

The control laws shown in the schematic are of a classical PID controller where the actuator force is derived from a linear combination of proportional, differential, and integral of the position error e :

$$e = (\text{Desired position}) - (\text{Measured position})$$

$$F_a = K_d \frac{de}{dt} + K_p e + K_i \int e dt \quad (4-20)$$

The differential term not only provides the necessary damping to the actuator itself, but also for the mirror/whiffle tree system as discussed in section 2.3.1. The integral term essentially provides infinite stiffness at zero frequency, i.e. it makes sure that the static error is exactly zero.

The typical error response of this type of system under external sinusoidal disturbance is shown in Figure 4-3. It starts from zero when the disturbance frequency is zero, and reaches a maximum around the bandwidth of the control system. Above the bandwidth frequency, the control system itself becomes ineffective, however the inertia forces (mirror mass in this case) provide an increasing attenuation with frequency (response proportional to $1/f^2$).

The parameters chosen for this example correspond to a 30 Hz control bandwidth and 10 N/ μm for the rigid system stiffness. (the whiffle tree stiffness is assumed infinite in this case so that mirror and actuator motions are the same).

The closed-loop error function plotted in Figure 4-3 is given by the expression:

$$G_{cl}(u) = (F_d / M \omega_b^2) j u / [(1 + j u) (2 + 2 j u - u^2)] \quad (4-21)$$

where: ω_b is the control bandwidth (rad/s)

$$u = \omega / \omega_b$$

and the control gains of Eq. 4-21 are chosen as:

$$K_d = 3 M \omega_b, \quad K_p = 4 M \omega_b^2, \quad K_i = 2 M \omega_b^3$$

The rigid response is calculated as:

$$G_r(u) = (F_d / M) / [\omega_r^2 + 2j \zeta \omega_r \omega - \omega^2]$$

where: ω_r is the structural resonance frequency (rad/s),

$$\omega_r^2 = K_r / M, \quad K_r \text{ is the stiffness of the actuator.}$$

As can be seen in this example, the bandwidth of the control system can be adjusted to provide an equivalent stiffness satisfying the original requirement at all frequencies (as in this example). However, at frequencies lower than the bandwidth, the controlled actuator shows significantly superior performance. The complete control system, which includes the offloading system, is shown in Figure 4-4.

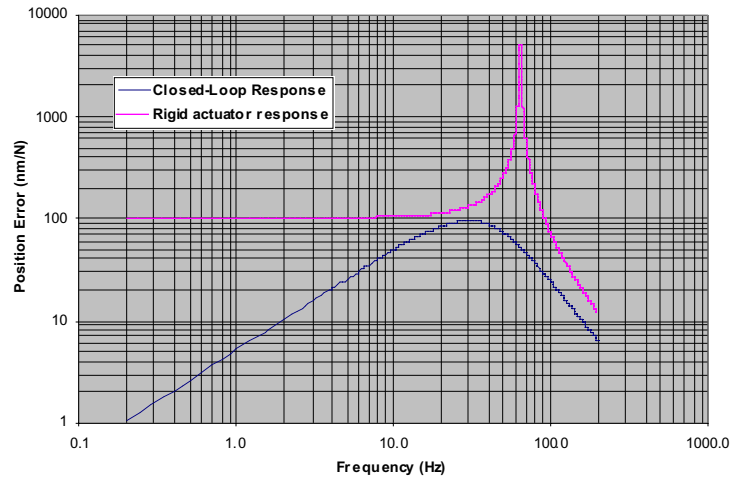


Figure 4-3 PID Controller vs. Rigid Actuator Response

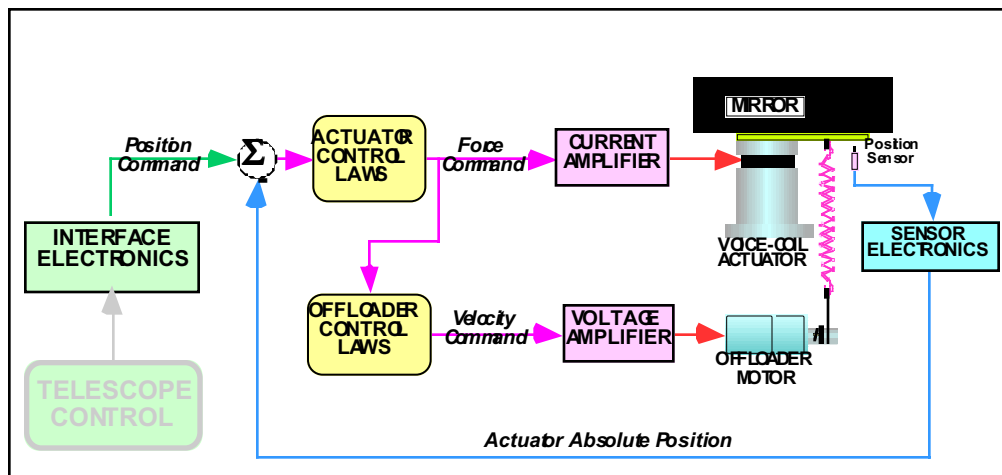


Figure 4-4 Overall Mirror Actuator Control system

The control laws for the offloader motor simply use the command to the voice-coil actuator as control error. Although the implementation of these laws uses discrete elements (current switch), in an average sense the motor speed becomes proportional to the error, thus driving the error to zero.

The output of the offloader motor is ultimately the linear displacement x such that :

$$(4-22) \quad x = \Delta_0 \theta / 2\pi, \quad \text{where } \theta \text{ is the motor shaft angle.}$$

The motor rate is essentially proportional to the input voltage (because of back emf). We will assume that this voltage can be made proportional to the force F_c commanded to the voice coil actuator. The offloader control law is thus:

$$d\theta/dt = G_o F_c \quad (4-23)$$

where the gain G_o depends upon the voltage amplifier gain and the motor gain. Because the current amplifier has a relatively high bandwidth, it can also be assumed that the actual actuator force $F_a = F_c$. The output of the offloader is thus :

$$dx/dt = (\Delta_o G_o / 2\pi) F_a \quad (4-24)$$

At low frequencies where the offloading system operates , for a quasi-static force F_d applied to the actuator, the dynamic equations of the full system are:

$$F_a = F_d + K_s (z - x) \quad (4-25)$$

using (4-23) one obtains:

$$dx/dt + (\Delta_o G_o K_s / 2\pi) x = (\Delta_o G_o / 2\pi) (F_d + K_s z) \quad (4-26)$$

Since the spring constant K_s is known, as well as the integral gain K_i and the motor gain Δ_o , the control design must choose a value for G_o which maintains the residual force F_a below an acceptable level. The bandwidth of the offloading system can be calculated from Eq. 4-26 and is given by:

$$\omega_{off} = \Delta_o G_o K_s / 2\pi \quad (4-27)$$

The actuator force differential equation is then given by:

$$dF_a/dt + \omega_{off} F_a = dF_d/dt \quad (4-28)$$

If the disturbance force varies with time (e.g. gravity vector change), then the residual actuator force is given by :

$$F_{res} = (dF_d/dt) / \omega_{off} \quad (4-29)$$

Conversely this equation is used to determine the minimum bandwidth ω_{off} , given a maximum residual force:

$$\omega_{off} = (dF_d/dt) / F_{res} \quad (4-30)$$

Given that dF_d/dt is about $29.4 \text{ N} / (6 \times 3600) \text{ s} = 0.0013 \text{ N/s}$, to maintain for example a residual force of 0.002 N in the actuator will require a bandwidth of about 0.1 Hz .

To achieve this 0.1 Hz bandwidth the gain G_o must then be (from Eq. 4-27):

$$G_o = 0.1 * 2\pi * 2\pi / (6.3 \times 10^{-5} * 490) = 128 \text{ rad/s/m}$$

4.5 Performance evaluation

This section evaluate the predicted performance of the proposed CSPA using the choices for the design parameters presented in section 4.4.

The following parameters have been chosen for the baseline design:

Parameter	Value	Units
Mirror mass (per actuator)	25	Kg
Actuator mass (includes whiffle tree)	5	Kg
Counterweight mass (minimum)	1	Kg
Position sensor noise equivalent	3.6	nm
Actuator stroke	1.2	mm
Actuator power constant	5	N/W ^{-1/2}
Actuator bandwidth	100	Hz
Offloader spring constant	490	N/m
Offloader gear ratio	2400:1	
Offloader shaft radius	10	mm
Offloader bandwidth	0.1	Hz

Table 4-2 Baseline design parameters

4.5.1 Mirror Position Accuracy

The mirror positioning accuracy is essentially a function of the sensor noise and of the disturbance acting on the mirror.

The capacitive sensor chosen for this design will be capable of measuring up to 1.2 mm with an equivalent output noise below 4nm. The dynamic range of 300,000:1 is relatively large but not uncommon (e.g. Keck edge sensors) and is achievable by selecting proper electronic components. This kind of sensor is very stable and has low sensitivity to temperature. The sensitivity is mostly in the electronics which will be designed to maintain a stability better than 7 nm in 20 minutes.

The major challenge for the CSPA is to properly handle external disturbances, the largest of which is the residual wind blowing on the primary through the dome aperture. Although no direct data is available at this time to quantify the effect of the wind, results obtained for the Keck telescope are used in this report to obtain an estimate of the mirror position error.

A wind spectrum was derived from actual wind velocity measurements on Mauna Kea in 1992. The corresponding wind pressure rms as a function of frequency is given by the expression:

$$P(\omega) = 0.5 / \text{sqrt}(\omega_0^2 + \omega^2) \quad (4-31)$$

where $\omega_0 = 2\pi$ (1/2 Hz).

The static pressure on a 1 m² segment results in about 1N of force. This corresponds to a 14 m/s wind velocity outside the telescope, reduced by a factor ten inside the dome. (The classical drag term $0.5 \rho v^2 \sim 0.5 (1.4)^2 \sim 1$ N). As the frequency increases the disturbance force decreases in a manner shown in Eq. 4-31.

Because there are 3 actuator per segments, each actuator only sees one third of the disturbance, and only one third of the mass of the mirror/whiffle tree system. Given the control system described in section 4.4 with a control bandwidth of 30 Hz, and assuming a rigid whiffle tree, one can calculate the response of the mirror (as seen by each actuator) as a function of frequency. These results are displayed in Figure 4-5 where the total mirror response is plotted along with the actuator error function and the wind spectrum. Numerical results indicate that the motion stays below 2.3 nm at all frequencies.

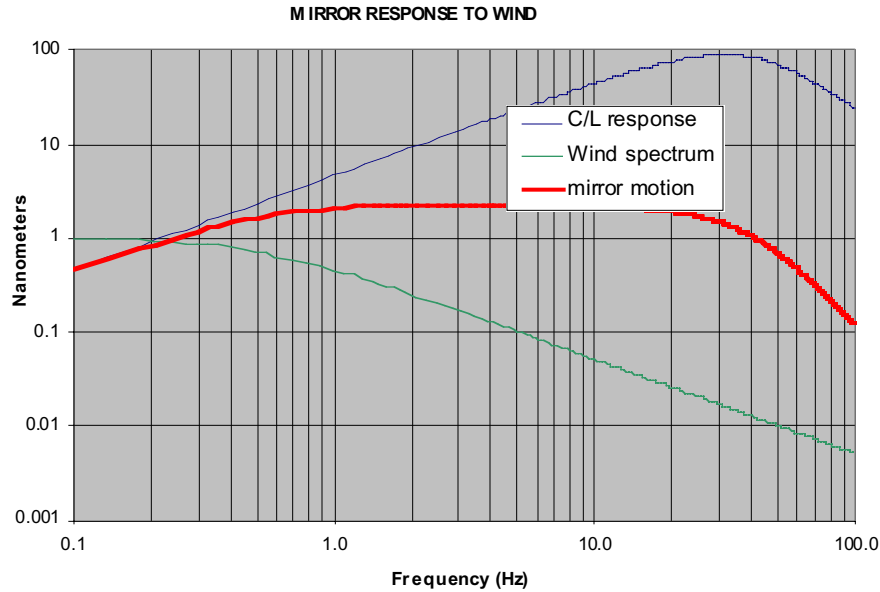


Figure 4-5 Mirror Response to Wind Disturbance - Rigid Whiffle Tree Case

Performance with a flexible whiffle tree

For the actual CELT design, the whiffle tree is not rigid but behaves like a spring between the mirror and the actuator. A similar, but more complex analysis shows that an higher actuator bandwidth is required to provide the necessary damping of the system. The unfortunate effect of the flexible whiffle tree, is that its quasi-static response stays around 100 nm/N, even for a perfectly controlled actuator. With a rigid actuator satisfying the 10 N/ μ m stiffness requirement, this number is doubled since the stiffness of both systems are in series.

Figure 4-6 shows the response of the actuator with 100 Hz bandwidth and a whiffle tree of 10 N/ μ m stiffness (corresponding to about 60 Hz resonance of the mirror/whiffle tree system). The parameters used are those of table 4-2.

The damping effect of the actuator can be seen clearly (blue curve), and the analytical result shows also that the response at low frequency is dominated by the springiness of the whiffle tree.

The response of the actuator alone (when not attached to the mirror/whiffle tree system) is also shown in Figure 4-6 and a typical of a PID type control system. When the mirror/whiffle tree system is attached, the two resonant modes of that system show up as zeros (green curve).

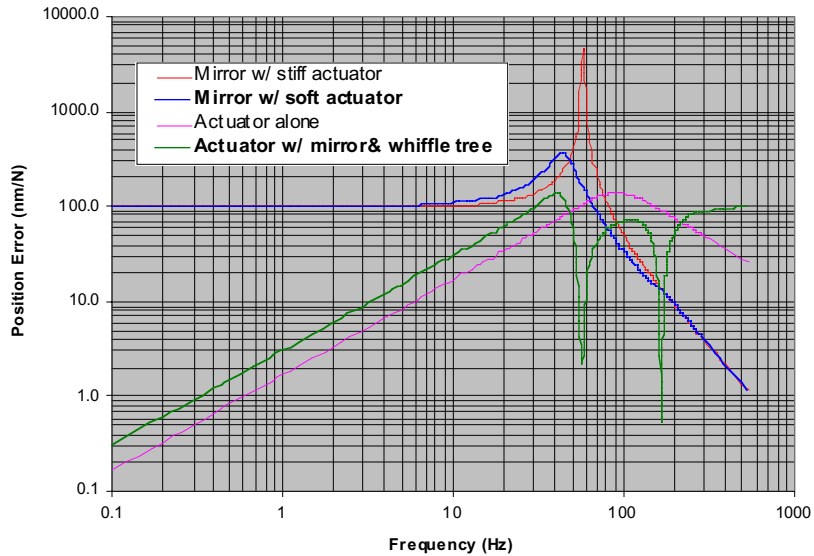
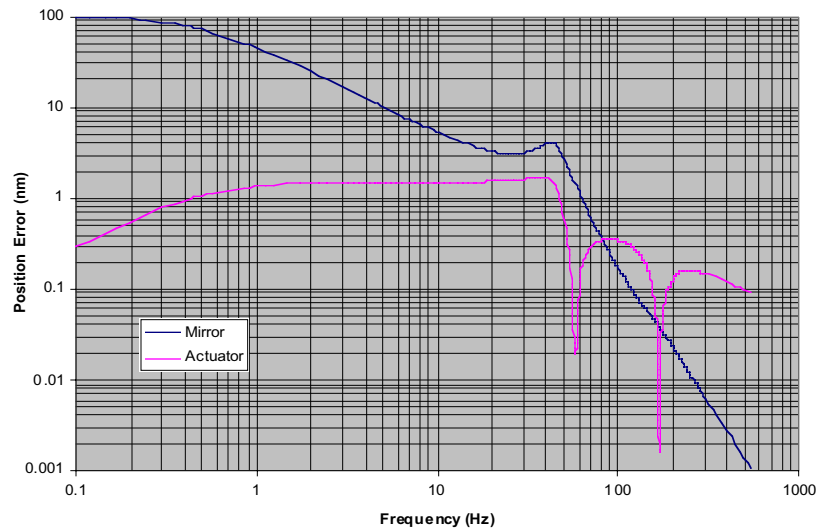


Figure 4-6 Responses to External Disturbance - Flexible Whiffle Tree Case

The values chosen for the bandwidth and damping of the actuator control system correspond to an optimum condition for damping the mirror/whiffle tree system and still getting acceptable position performance.

Performance under wind conditions

Using the wind model described by Eq. 4-31 one can estimate the response of the mirror and the actuator output shaft position at various frequencies. A plot of these results is shown in Figure 4-7. The actuator position clearly meets or exceeds the requirements by staying below



2 nm. The

Figure 4-7 Estimated responses to Wind Disturbance

mirror position however is again driven by the flexibility of the whiffle tree system, but the effect of the spring/mass resonance at 60 Hz is properly damped and does not significantly affect the overall performance.

Performance under offloading conditions

When the offloader motor is activated, it essentially compress or expand the offloading spring by a small amount δs resulting in a perturbation force δf on the mirror:

$$\delta f = K_s \delta s$$

For this evaluation, it is assumed that the motor minimum motion is a full turn, therefore producing a displacement:

$$\delta s = \Delta_o = 2 \pi R_s / G_r = (2 \pi) (0.01) / (1000) = 62.8 \cdot 10^{-6}$$

The incremental force on the mirror is thus:

$$\delta f = K_s \Delta_o = (490) (62.8 \cdot 10^{-6}) = 0.03 \text{ N}$$

The actuator control system response to a step function (worst case) is given by:

$$\delta x = \delta f / (4 M \omega_b^2) = 0.03 / [(4) (5) (2 \pi 100)^2] \sim 7 \text{ nm}$$

This number seems to be at the limit of the requirements, however, because the motor has a limited rotation rate, the control system can attenuate the disturbance much more effectively, resulting in an error much less than 7 nm.

Even with a maximum rate of 6000 rpm (630 rad/s) the error from the PID controller is less than a nanometer:

$$\delta x = (630) \delta f / (2M \omega_b^3) = 630 * 0.03 / [(2) (5) (2 \pi 100)^3] < 1 \text{ nm}$$

Performance under tracking conditions

During normal operations, the telescope may be required to slew almost from horizon to Zenith to horizon (tracking). This means that the gravity load on the actuator can go from 0 to 30 Kg in 6 hour, corresponding to 29.4 N at the offloader spring. Since the spring maximum extension is 60 mm, the corresponding motor rate is:

$$\Omega_{\text{track}} = (2 \pi) (0.06) / \Delta_o / (21600) = 0.06 / (62.8 \cdot 10^{-6}) / 21600 = 0.3 \text{ rad/s}$$

Because of the deformation of the telescope under gravity loads, it may be expected that the actuator is actually required to move a maximum of 1.2mm from Zenith to horizon, while the offloader motor will have to follow to keep the actuator current near zero.

While the PID controller perfectly eliminates static errors, it only reduces tracking errors by some amount. The exact form of the position error (hang-off) due to a tracking rate V_{track} is given by:

$$\delta x_t = V_{\text{track}} / (2 \omega_b) \quad (4-32)$$

since $V_{\text{track}} = 0.06 / 21600 = 2.78 \mu\text{m/s}$,

the estimated hang-off error is:

$$\delta x_t = 2780 / (400 \pi) = 2.2 \text{ nm}$$

Note that this number is very conservative since it does not assume any offloading mechanism, but purely the action of the control system.

Performance under slewing conditions

During a slew, although there is no requirement for observing, the rate is much higher since the telescope must go from Zenith to horizon in 2 minutes. The motor speed is then:

$$\Omega_{\text{slew}} = (2 \pi) (0.06) / \Delta_o / (120) = 0.06 / (26 \cdot 10^{-6}) / 120 = 120 \text{ rad/s } (<1200 \text{ rpm})$$

This is well within the capability of the motor.

4.5.2 Power Dissipation

The power dissipated by the voice coil actuator is very dependent on the environmental and observing conditions. If the system is absolutely quiescent, there is a residual excitation of the actuators due to sensor noise coming back from the feedback loop. Then there is the actuator noise itself, due to the drive electronics. Then, if there are any dynamic perturbations to the system, the actuators have to react to the disturbance forces by applying counter forces, thus dissipating even more power.

In the following analyses it is assumed that the actuator power constant C_p is 5 N /root(W).

Sensor noise conditions

The sensor noise s_n is estimated to be about 3.5 nm rms within a bandwidth ω_s of about 6000 rad/s. The corresponding mean square force generated by the PID control system is given by:

$$\langle \delta f_{\text{sn}}^2 \rangle = \langle s_n^2 \rangle (M^2 / \omega_s^2) p(\omega_b)$$

where

$$p(\omega_b) = \int [(4\omega_b^2 \omega)^2 + (2\omega_b^3 - 3\omega_b \omega^2)^2] \omega^4 / [(4\omega_b^2 \omega - \omega^3)^2 + (2\omega_b^3 - 3\omega_b \omega^2)^2] d\omega$$

The integral is taken from 0 to ω_s and the rms force is calculated as:

$$\delta f_{\text{sn}} = 0.014 \text{ N}$$

Actuator noise conditions

To calculate the actuator noise it is assumed that the drive electronics has at least a 60 dB signal-to-noise ratio, thus for a the maximum force produced by the actuator of 5 N, the rms force fluctuation in the actuator will be:

$$\delta f_a = 0.005 \text{ N}$$

Wind conditions

As seen in the previous section, the wind force on the actuator portion of the mirror is at most 0.333 N. If one assumes that the control system is perfect and exactly oppose this force, then an upper bound for the rms actuator force due to wind is:

$$\delta f_w = 0.033 \text{ N}$$

Tracking conditions

Using the value of the hang-off error calculated previously (i.e. 2.2 nm) it is possible to determine the actuator force necessary to fight the offloader spring. The estimate is thus:

$$\delta f_t = K_s \delta x_t = (490) (2.2 \cdot 10^{-9}) = 1.08 \cdot 10^{-6} \text{ N}$$

a very negligible contribution indeed.

Total power dissipation in the actuator

The total nominal power dissipated in the actuator is obtained by taking the sum squares value of the preceding contributions and applying the power factor:

$$P_{\text{total}} = (\delta f_{\text{sn}}^2 + \delta f_{\text{a}}^2 + \delta f_{\text{w}}^2 + \delta f_{\text{t}}^2) / C_p^2 = 0.0013/25 = 0.0524 \text{ mW}$$

For a coil resistance of 2 Ohms, the corresponding current is about 5 mA. If the DC power supply for the actuator power amplifier uses $\pm 15\text{V}$, the power dissipated in the electronics due to actuator commands is then

$$P_e = 30 * 5 = 150 \text{ mW}$$

4.6 Electronic interface concept

This section presents a concept for commanding all the actuators from the telescope computer which is low cost, robust, and efficient while preserving the resolution and accuracy required.

The overall system is shown in Figure 4-8. The communication between the telescope control computer and the primary mirror actuators is implemented via a serial bus system with a tree structure to simplify cabling and addressing. When the telescope computer commands a move for a particular actuator, it sends two digital words on the bus. The first word is the address of the actuator (a 12-bit integer which is capable of handling over 4000 actuators), the second represents an incremental command (a signed 8-bit integer representing up to ± 128 nanometers of motion).

A main address decoder routes the messages to the different subsections of the primary mirror system. At the segment level, each actuator electronics has its own local decoder to catch the command pertinent to it. A 24-bit up-down counter keeps track of the absolute commanded position of the actuator which is then converted to an analog signal driving the actuator control system. This system preserves the nanometer resolution while providing ample dynamic range to cover the 1.2 mm stroke required from the actuator.

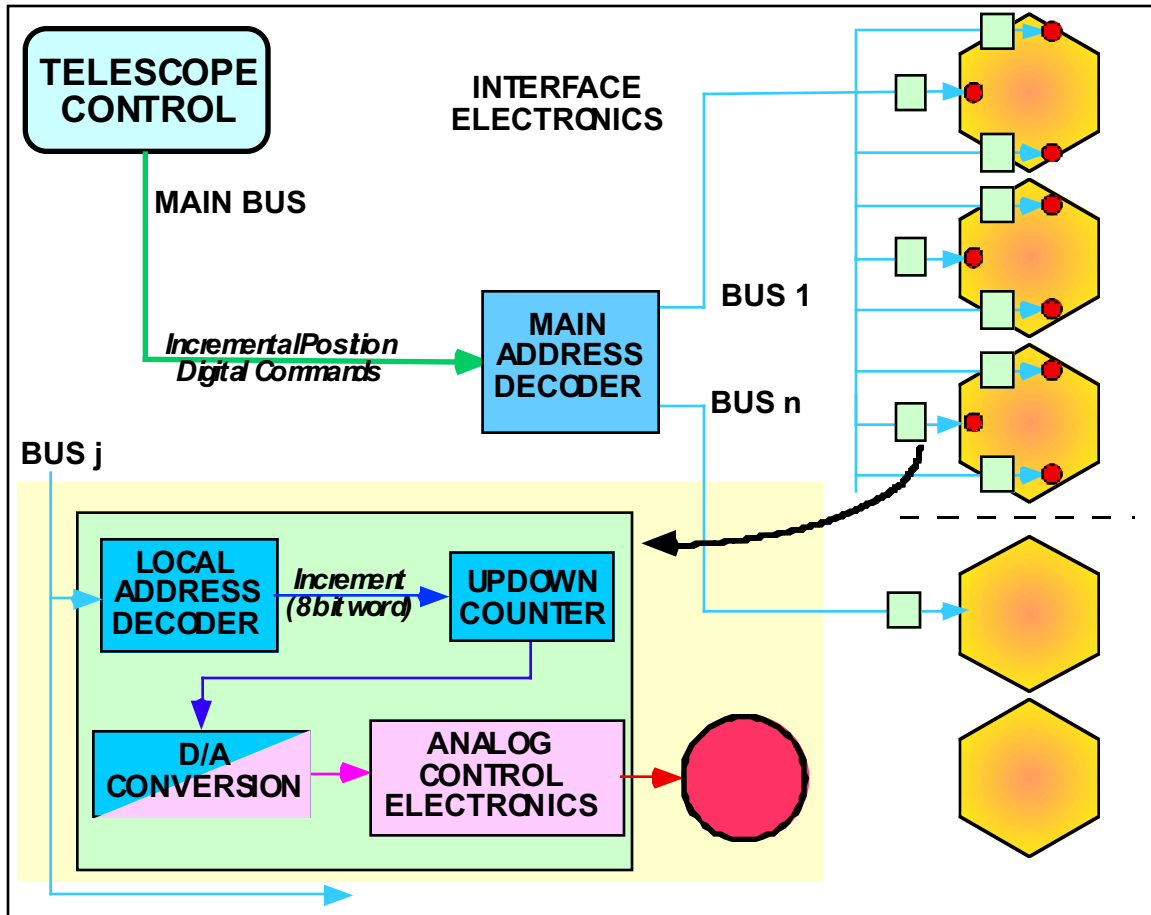


Figure 4-8 Distributed Serial Bus System Provides Commands to Each Mirror Actuator

4.7 Compliance Matrix

A summary of how the design of the CSPA satisfies the current CELT requirements is given in Table 4-3 below:

Requirement Description	Requirements	Design Approach
MECHANICAL		
<i>Physical Requirements</i>		
Body length	< 20 cm	Compact design fits in an 18 cm long cylinder
Body outer diameter	< 20 cm	Coaxial design fits inside a 14 cm diameter
Neck length	< 30 cm	Neck length can be built from 2 to 20
Neck outer diameter	< 6 cm	Steel tube can be built with 2 OD
<i>Stiffness Requirements</i>		
Transverse load capacity	> 5 Kg	Load taken by the neck disk flexures at both ends
Axial load capacity	> 30 Kg	Load supported through 10:1 stiff lever system by spring and possibly counterweight.
Transverse stiffness	> 0.1 N/μm	Achieved through neck disk flexures
Axial stiffness	> 10 N/μm	Achieved actively through voice-coil actuator and

		control system
Mechanical Accuracies		
Mounting accuracy	< 0.25 mm	Overall actuator position easily adjustable through neck sliding mount inside telescope structural node
Performance Requirements		
Range	> 1.2 mm	Compatible actuator stroke and levers capability
Rms. position error over 20 minutes	< 7 nm	Achieved through quality position sensor, low noise electronics and control system bandwidth
Slew rate	> 10 $\mu\text{m/s}$	Offloader gear ratio of 2400 requires only 1200 rpm input, well within motor capability
ELECTRICAL		
Local average power dissipation	< 2 W	Achieved through a very efficient actuator (over 5 N/root(W) and pulsed motor drive
Lifetime	> 10 Years	All flexural parts designed for low stress resulting in almost infinite life time. Robust, industrial type motor/gear box can run for billion cycles. Simple and robust electronic circuits with life expectancy exceeding requirements
ENVIRONMENT		
Survival temperature	-18 to +22 $^{\circ}\text{C}$	All parts can survive -50 to 50 $^{\circ}\text{C}$
Operating altitude	4300 m	Design contains no pressure sensitive elements
Operating temperature	-6 to +10 $^{\circ}\text{C}$	Mechanical design insensitive to thermal expansion Gear box lubricant designed for low temperature Electronics parts operational temperature range in excess of requirements
Operating humidity	1 to 100% condensing	Main mechanical system does not require lubrication an could work under water. Motor/gear box protected by lubricant.

Table 4-3 Requirements Compliance Matrix

5. Cost Estimate

ITEM	QUANTITY /actuator	Unit Cost	Cost /actuator	Total Cost for 4000 (in K\$)
Mechanical parts			510	2.04
Lever Flexure	3	100	300	
Disk Flexures	3	10	30	
Canister	1	10	10	
Actuator mount / counterweight	1	20	20	
Neck & shaft	1	50	50	
Miscellaneous	1	100	100	
Electro-mechanical			580	2,320
Voice-coil actuator	1	500	500	
Motor/ Gear Box	1	80	80	
Capacitive Sensor	1	10	10	40
Electronics			295	1,180
Sensor electronics	1	55		
Control loop	1	35		
Actuator Drive	1	30		
Clock & Power parts	1	175		
Assembly	1	200	200	800
Test /Check out /Packaging & Shipping	1	200	200	800
Contingency/Fees	1	400	400	1,600
Total	1		2195	8,780

6. Areas of Concern

The areas of concern for this program can be divided into two main categories; programmatic risk associated with schedule and budget, and technical risk associated with inability of the design to meet performance goals. Within the area of technical risk, there are two sub categories; risk associated with the design not meeting one or more requirements associated with positioning a segment, and risk that no matter how well the actuator performs, it has poor reliability. Although we have no real means of quantifying these three types of risk, it is certainly possible to address them in a qualitative way to at least understand the likelihood that one or more of these areas deserve serious further investigation.

6.1 Programmatic Risk

Schedule and budget risk is problems associated with any type of undertaking in which the responsible individuals attempt to predict the exact date of completion and the associated cost. Home remodeling and aerospace projects probably have the worst track record in our culture on these two issues. Unfortunately, the CELT has many features in common with a modern aerospace project including high technical content, long lead times for design and fabrication, and complex technical and management interfaces for a large number of subsystems. The segment positioning actuators probably have a lower overall schedule and budget risk than the larger project, but because there are so many units to fabricate, even a small design, component, or manufacturing problem is magnified by the sheer number of units and will cause an enormous perturbation in the schedule and budget. It is therefore strongly advised that sufficient margin for both schedule and budget be included for the segment actuators so that the success of the project will not have a critical dependence on the precise schedule and budgetary performance of the supply of actuators. With respect to schedule and budget, probably the highest uncertainty lies with the cost. Cost has a high uncertainty because at this early stage in the design it is very difficult to obtain accurate numbers from vendors and suppliers for large production runs of specific components. The only means of compensating for this risk is to add budget margin to protect against future surprises.

6.2 Technical Risk/Performance Goals

Of the three types of risk identified for the segment actuators, the risk of not meeting one or more performance goals is probably the lowest. Because the design developed in this study is well understood and utilizes well-known and proven technology to achieve the desired performance, it is our judgment that the design requirements will be met with very low risk. The design analyses performed in the preceding sections of this report confirm that the proposed concept has margin with minimal risk. The key component that will control the performance is the sensor. The dependence on sensor performance was identified from the beginning of the study and major engineering effort is being directed at producing a sensor design that meets both performance and cost goals. We believe that our sensor concept will meet or exceed requirements in both areas. The development of a prototype in the second phase of this study will confirm the design approach and provide a major step in the elimination of this part of the technical risk.

6.3 Technical Risk/Reliability

Although the proposed design has relatively few parts compared with a rigid actuator, there are several critical components that must be designed to a very low risk of failure

The principal mechanism essentially relies on a system of flexures that are compliant enough to permit motion about their soft axis, while providing the necessary stiffness in the transverse degrees of freedom. These flexures are attached to structural elements (beams, bars, tubes etc.) that are considerably stronger. Thus they constitute the weaker part of the link and must be designed to withstand not only the static load (with some comfortable safety margin), but also the fatigue resulting from alternating strain.

There are a total of 6 flexures in the proposed design, 3 disk and 3 blade flexures. The disk flexures are under relatively low stress conditions, only supporting the side loads from the whiffle tree but not the full mirror weight (neck disk flexures) or the weight of the counterweight (canister disk flexure).

The flexures in the lever system are under more stress because they do carry the full load of the mirror/whiffle tree system. The design is such that these flexures are almost always under tension so there is never a possibility of buckling damage. Their length and thickness are calculated to keep the cyclic bending stress at a level well below yielding to ensure a quasi-infinite lifetime.

Flexural systems have been proven very reliable in the Keck 1 and 2 infrared chopping secondary mechanisms and the Gemini M2 systems. They do not represent, in our opinion a real risk to the system.

The rest of the mechanism includes a DC motor and gearbox system, which is used routinely in many industries (e.g. robotics) and is considered highly reliable. However, it has only a limited lifetime, defined essentially by the number of turns of the motor. Contamination of the brush system or the gearbox is usually the cause for accidental failure.

The electronics subsystem has been intentionally designed to be very simple too, with a small number of parts. The elements presenting the most risk are the power transistors that could possibly overheat given enough current. Limiting current commands and sizing the power supply voltage minimizes this risk.

The development of a prototype actuator, as discussed in the preceding section, will be a major contribution to understanding the risk associated with reliability. It is our strong recommendation that a comprehensive lifetime and reliability test with one or more prototype actuators be initiated in order to gain an understanding of where the weak points of the design are. On-going results of this type of testing will allow engineering effort to be directed at these weak areas so that cost-effective solutions can be developed and incorporated into the test articles. Under no circumstances should production be initiated until pre-production prototypes have been thoroughly tested and proven.

7. Conclusions and Recommendations

An actuator design has been developed for the California Extremely Large Telescope that meets all the requirements and provide additional value to the telescope operation by introducing damping in the structure.

The design is based upon the combination of a voice coil actuator that provides the fine positioning and an automatic offloading system. This technique provides the necessary force to balance the weight of the mirror at all elevations. A high level of performance is obtained by a control system that adjusts the current in the voice coil actuator based upon the readings from a very accurate capacitive position sensor. The control laws create equivalent stiffness and damping properties that are necessary to achieve high positioning accuracy even in the presence of external disturbances such as wind.

The mechanical design of positioning system contains no bearings, bushings or friction sensitive devices, and is entirely based on flexural elements. It utilizes a lever reduction system that significantly reduces the power consumption and weight of the system.

Several options have been considered and the final selection consists of an actuator in which the weight of the mirror is offloaded partially by a counterweight, partially by a motor-driven spring (offloader). Because the best combination of these two means of offloading is not completely known at this time, from full counterweighting to full motor offloading, this hybrid design offers flexibility for future adjustment.

The proposed design is self-contained and can be removed in its entirety from the telescope by sliding the neck part out of the telescope support structure node. The electronics and offloading system can be accessed and serviced from the bottom and side of the without removing the actuator from the telescope.

Although this type of design has been used successfully in a number of applications, including secondary mirrors for telescopes such as Keck 1 and 2 and the two Gemini telescopes, we strongly recommend that a prototype be built and tested to evaluate its performance and reliability, and optimize the way in which counterweighting and active offloading should be combined.